Isotherm, Kinetic and Thermodynamic Studies of Adsorption of Naphthol Blue Black-B Dye from Aqueous Solution using Synthesised Copper Oxide Nanoparticles

Saraswathi G.* and Vasuki M.
PG and Research Department of Chemistry, Seethalakshmi Ramaswami College, Tiruchirappalli, Affiliated to Bharathidasan University, Tiruchirappalli, Tamil Nadu, INDIA
*saraswathig7@gmail.com

Abstract
The present research work examined the elimination of Naphthol Blue Black –B dye from aqueous solution by the use of copper oxide nanoparticles as suitable adsorbent. The nanoparticles that were synthesised, were characterised by using FTIR, SEM, EDX and XRD techniques. Studies on batch adsorption were performed by varying factors such as contact period, adsorbent dose, dye concentration, pH, speed of agitation, temperature and desorption studies.

Batch adsorption results were explained by applying isotherms like Freundlich, Langmuir, Dubinin-Raduskevich, Temkin and Jovanoic models. Kinetic data suggested that the batch mode experiment obeys pseudo second order kinetic model. Examination of thermodynamics indicated that the process of adsorption is feasible and spontaneous.

Keywords: Adsorption, Dye removal, Nanoparticles, Naphthol Blue Black-B.

Introduction

Industrialisation has been associated to environmental deterioration because of poisonous and hazardous effluents[3]. Dyes are major contributors towards environmental pollution due to drastic growth of industries[8]. They are highly toxic, carcinogenic and lead to serious health issues. They also affect photosynthesis and disturb the aquatic system[9]. It is difficult to remove dyes using conventional procedure due to their structural complexity[21].In the textile industry, Naphthol Blue Black-B is a common acidic diazo dye used to colour wool, nylon and silk. It causes many harmful effects in human beings such as irritation of eyes and respiratory system.

Therefore, it is essential to eliminate naphthol blue black-B dye before being discharged into aquatic system. Many treatment strategies have been applied to get rid of dyes from contaminated water like photodecomposition[19,24], electrolysis[28] and oxidation[5]. Adsorption is widely used because of its great efficiency, simplicity and low cost[33]. Recently metal oxide nanoparticles have substantial pollutant binding capacity owing to its small size, active surface and high porosity[15,16]. These particles are more effective adsorbing materials than conventional ones because of their unique characteristics, high reactivity and catalytic potential[36]. In the current investigation, elimination of naphthol blue black-B dye from solution using copper oxide nanoparticles was studied.

Material and Methods

Materials: Copper sulphate pentahydrate was purchased from Merck Life Science Pvt. Ltd., Mumbai. Sodium hydroxide and naphthol blue black-B dye were bought from Nice Chemicals Pvt. Ltd., Cochin.

Synthesis of copper oxide nanoparticles: Copper sulphate solution was prepared and kept in a magnetic stirrer at a speed of 500rpm. 0.5M sodium hydroxide solution was added drop by drop with continuous stirring. The stirring proceeded for 1 hour and temperature was maintained at 50-60°C until precipitation completed. It was filtered, thoroughly washed using distilled water, kept in an oven and dried for six hours at 100°C[25,30].

Characterisation: SEM study (Zeiss) was used to investigate the morphology of the synthesised adsorbent. The elemental analysis was performed using EDX (Oxford instruments). Using a MAPADA-UV (1100) spectrophotometer, the concentration of dye was determined. The FT-IR (Jasco - 5300) spectrometer was used to record the IR bands between 400 and 4000 cm^{-1} wave number. PXRD analysis was done using Malvern Panaltical diffractometer.

Adsorption studies: Dye solution (100ml) of concentration 15 mg/Land 0.05g of copper oxide nanoparticles was taken in Pyrex bottle kept in an orbital shaker and agitated at a speed of 250 rpm. The MAPADA-UV (1100) spectrophotometer was used to determine absorbance of dye solution at λ_{max} of 618 nm. The percentage removal[5] of the dye was found by the equation (1):

$$\% \text{ removal} = \frac{(C_0 - C_e)}{C_0} \times 100 \qquad (1)$$

C_0 and C_e are initial and final dye concentrations.

Results and Discussion

FTIR studies: FTIR spectra (Figure 1) of copper oxide nanoparticles before dye adsorption indicated a band at 517.0 cm^{-1} which is due to vibrations of Cu-O bond[7]. A broad absorption peak found at 3458.85 cm^{-1} is due to hydroxyl

group stretching of moisture content[27]. Figure 2 shows the FTIR spectra of the adsorbent after adsorption. It was observed that some peaks are shifted which confirmed the adsorption of dye over the adsorbent.

SEM Analysis: Figure 3 indicates the SEM picture of the adsorbent before adsorption which shows porous and well dispersed surface that facilitates adsorption[11]. Once the adsorption has taken place, the surface of the adsorbent becomes saturated with dye molecules (Figure 4).

EDX Analysis: Figure 5 represents the EDX spectrum of copper oxide nanoparticles. The spectrum shows the presence of copper and oxygen. No other impurity was detected. Thus the formation of copper oxide was confirmed[14].

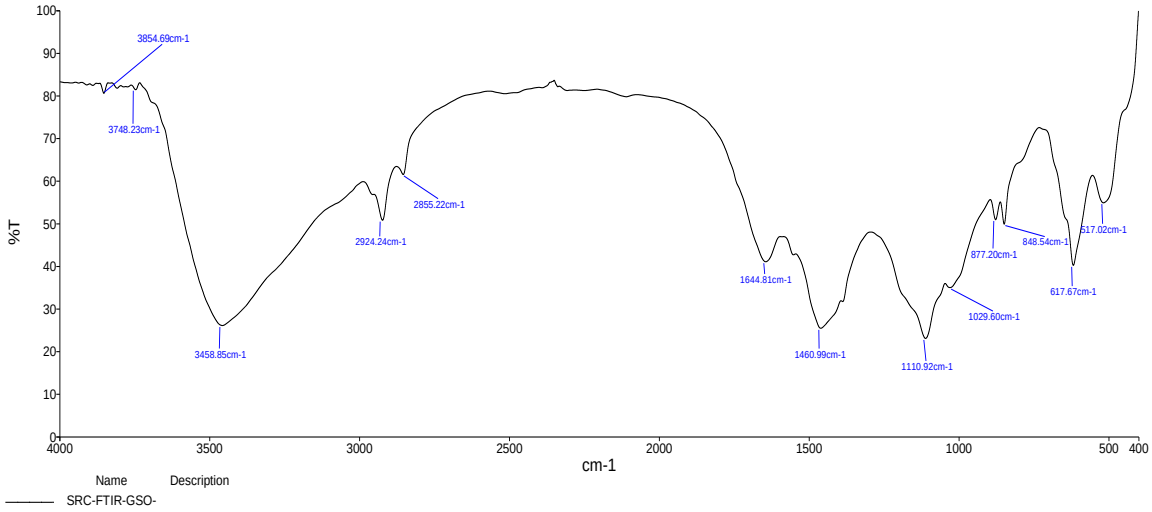

Figure 1: FTIR spectra of adsorbent before adsorption

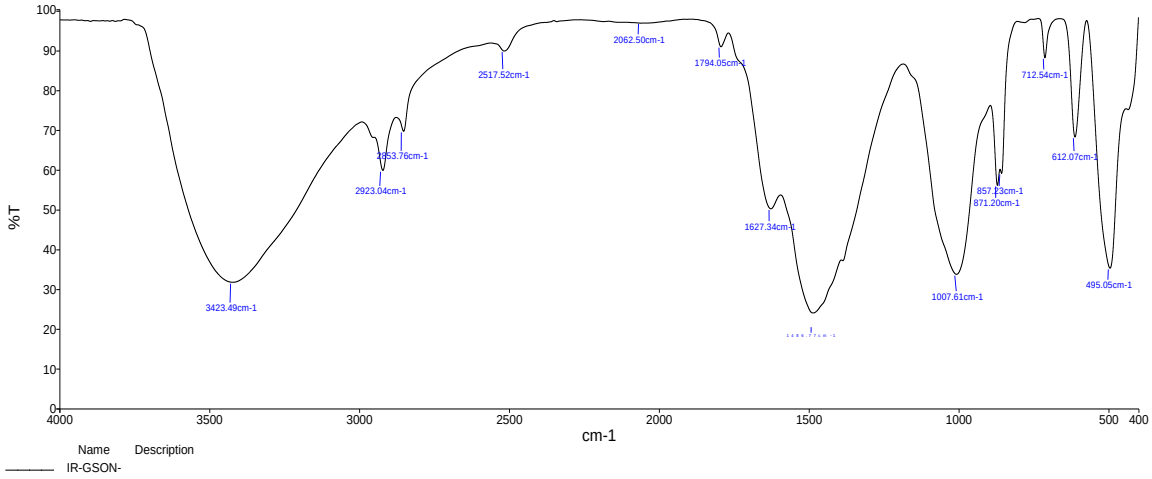

Figure 2: FTIR spectra of adsorbent after adsorption

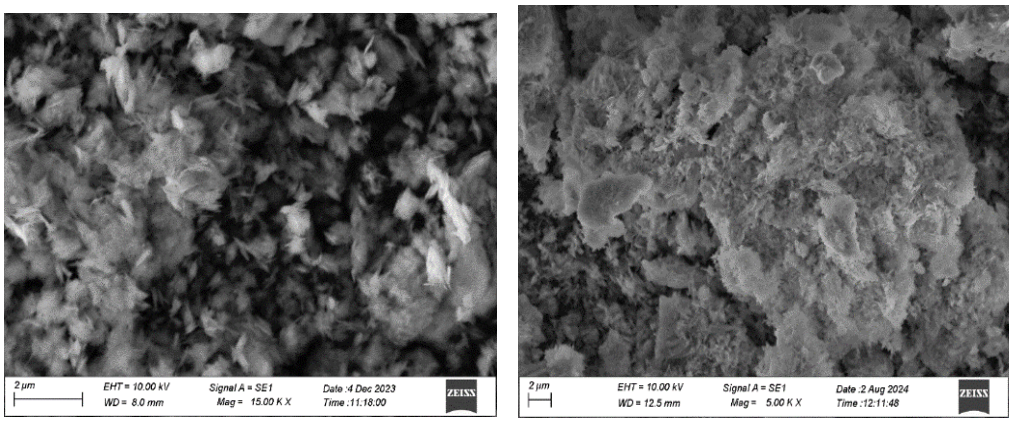

Figures 3 and 4: SEM image of copper oxide nanoparticles before and after adsorption

PXRD Analysis: PXRD analysis (Figure 6) of copper oxide nanoparticles showed diffraction peaks at 32.9º, 36.1º, 39.1º, 49.4º, 53.8º, 58.7º, 61.9º, 66.8º, 68.6º which may be due to the (110), (002), (200), (202), (020), (202), (113), (311) and (220) planes. These revealed copper oxide nanoparticles were in monoclinic phase (JCPDS 00-45-0937)[1].

Batch Mode Experiments

Variation of contact period: The influence of contact period on adsorption is investigated by altering it from 10-70 minutes taking dye solution (15mg/L) with 0.5g/L of adsorbent and shaken at 250rpm (Figure 7). The adsorption rises with increase in time of contact and then reaches equilibrium. The enhanced adsorption in the beginning stage might be due to the high number of active places which decreases as these sites are gradually occupied[18].

Variation of weight of adsorbent: Dye solutions (15mg/L) containing various adsorbent weights (0.1–0.9 g/L) agitated at 250 rpm are used to evaluate the influence of adsorbent on dye elimination. The outcome of the experiment was shown in figure 8. It was revealed that increase in amount of adsorbent dosage increases removal efficiency which might be due to large number of active spots for adsorption[4].

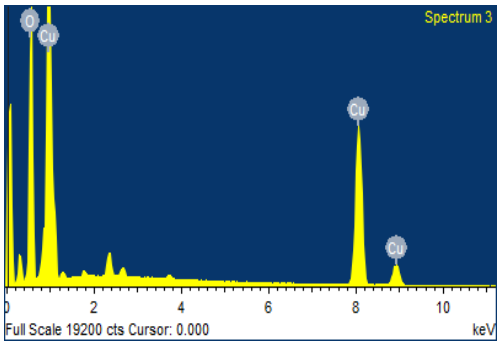

Figure 5: EDX Spectrum of copper oxide nanoparticles

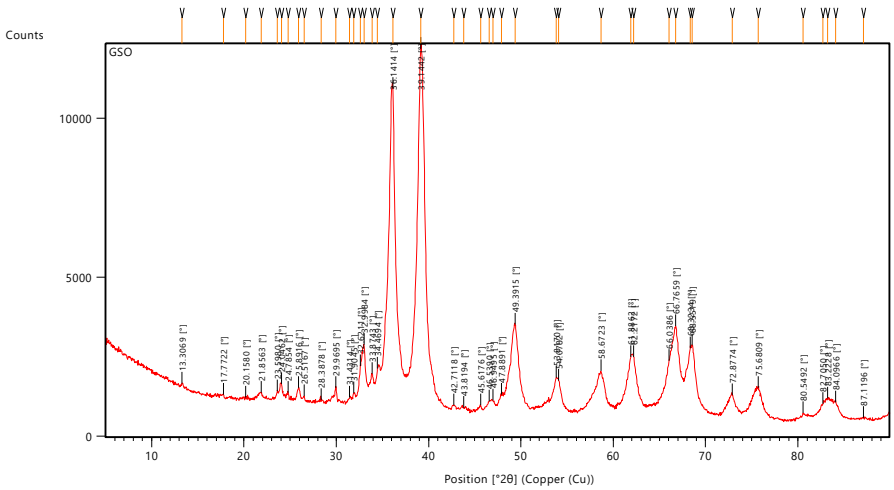

Figure 6: PXRD analysis of the adsorbent

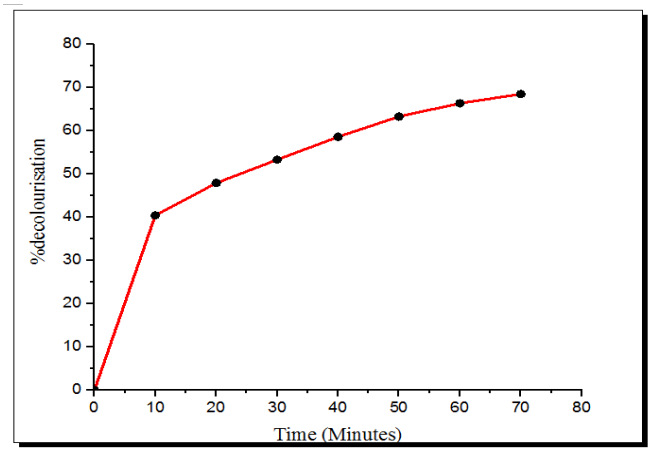

Figure 7: Variation of Contact time

Variation of concentration of adsorbate: Examination of concentration of adsorbate on decolourisation was performed by changing concentration of dye (10-20 mg/L) at adsorbent dose of 0.5g/L. Figure 9 shows the percentage decolourisation diminish as the concentration of dye rises. This might be because the active site on the adsorbent's surface becomes saturated with dye molecules[6].

Variation of pH: Impact of pH on percentage decolourisation has been examined at pH values of 4, 7 and 10 maintaining dye concentration of 15mg/L and adsorbent dose of 0.5g/L shaken at 250 rpm. The results are depicted in figure 10. It was noticed that adsorption increases as pH decreases. As the pH of the solution rises, fewer positively charged sites are present which result in less anionic dye adsorption[22].

Variation of Temperature: A plot of percentage decolourisation as function of temperature is shown in figure 11. The influence of temperature at 303 K, 308K and 313K was carried out by taking dye solution (15mg/L) at 0.5g/L dose of adsorbent and shaken at 250rpm. The data showed a high dye uptake with rise in temperature. This is associated with the high mobility of dye molecules and enables it to penetrate further[32].

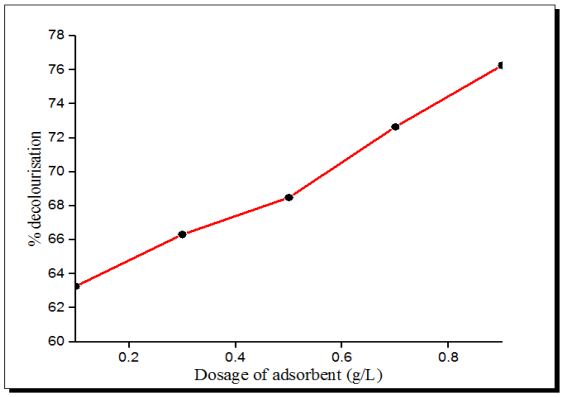

Figure 8: Variation of dosage of adsorbent

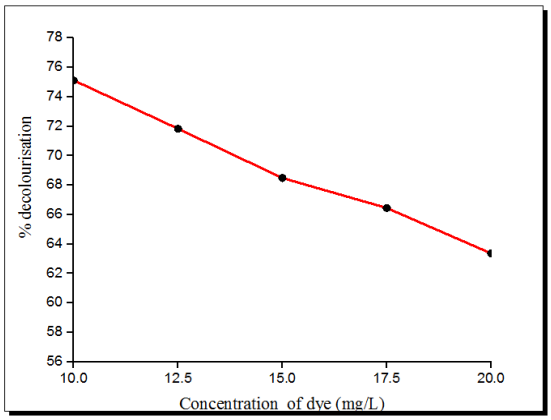

Figure 9: Variation of Initial Dye Concentration

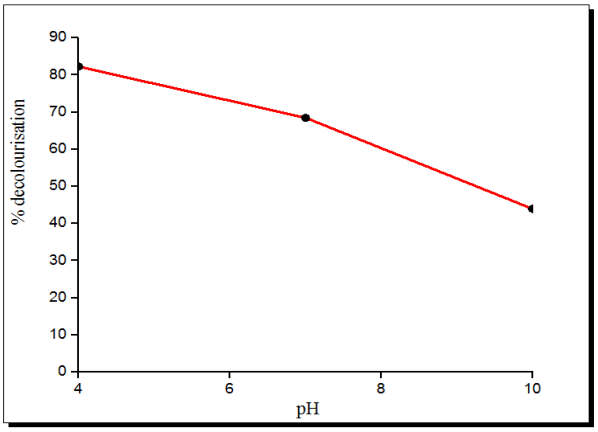

Figure 10: Variation of pH

Variation of speed of agitation: The influence of rate of agitation on percentage decolourisation was investigated by altering the rpm at 50,100,150,200 and 250 rpm maintaining other variables constant. Figure 12 indicated that agitation speed was found to increase the adsorption of dye because of decrease in boundary layer thickness due to high agitation speed[20].

Desorption Study: Reusability of the adsorbent is an essential factor in adsorption process since it makes it more economical. In this study, NaOH (0.1N-0.5N) was used as a desorbing agent. The results (Figure 13) revealed that percentage decolourisation increases with rise in concentration of NaOH which may be due to ion substitution[13].

Adsorption isotherm: The isotherms are employed to determine the relationship between the adsorbate concentration in the bulk at equilibrium and the amount adsorbed at the surface[1]. In order to verify the validity of the adsorption results, many isotherm models were applied.

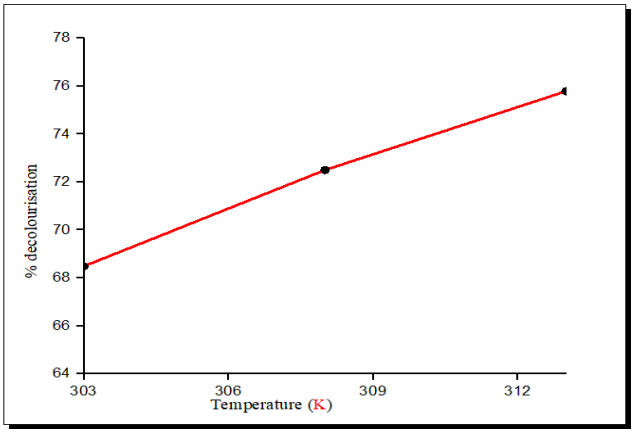

Figure 11: Variation of Temperature

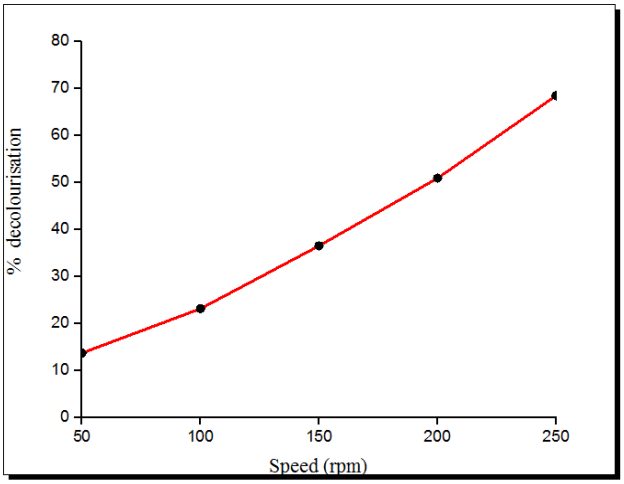

Figure 12: Variation of agitation speed

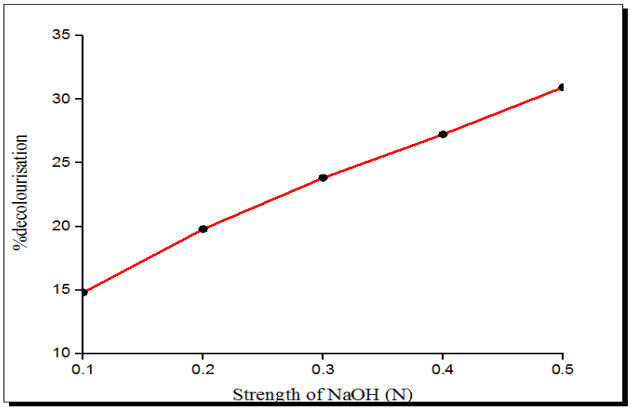

Figure 13: Desorption Study

Freundlich Isotherm: It is regarded as a multilayer adsorption as it depends on adsorption over a heterogeneous surface with different adsorption energy[2]. It is represented by

$$\ln q_e = \ln K_f + \frac{1}{n}\ln C_e \quad (2)$$

If $0 < \frac{1}{n} < 1$, the adsorption is favourable. The plot of In q_e Vs In C_e is linear. Figure 14 shows that adsorption data fitted well the Freundlich isotherm.

Langmuir Isotherm: It is used to represent the single layer adsorption[26]. The Langmuir equation in linear form is given by

$$\frac{C_e}{Q_e} = \left(\frac{1}{Q_0 b}\right) + \left(\frac{C_e}{Q_0}\right) \quad (3)$$

Where Q_0 is maximum dye uptake and b is Langmuir constant. The isotherm (Figure 15) fitted well on adsorption data. The dimensionless adsorption constant R_L[10] in Langmuir isotherm can be represented as:

$$R_L = \frac{1}{(1 + bC_i)}$$

In this experiment, the value of R_L was found to be 0.1613 which is in between 0 and 1 suggesting favourable adsorption.

Temkin Isotherm: It examined how interactions between the adsorbate and indirect adsorption affected the adsorption process[17]. It is expressed as follows:

$$q_e = B_T \ln K_T + B_T \ln C_e \quad (4)$$

The plot of *In* C_e Vs q_e (Figure 16) is linear which showed that experimental data fitted Temkin isotherm well.

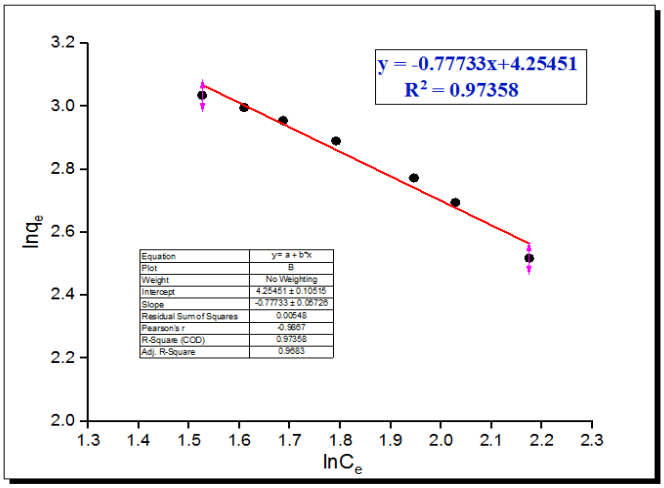

Figure 14: Freundlich Isotherm

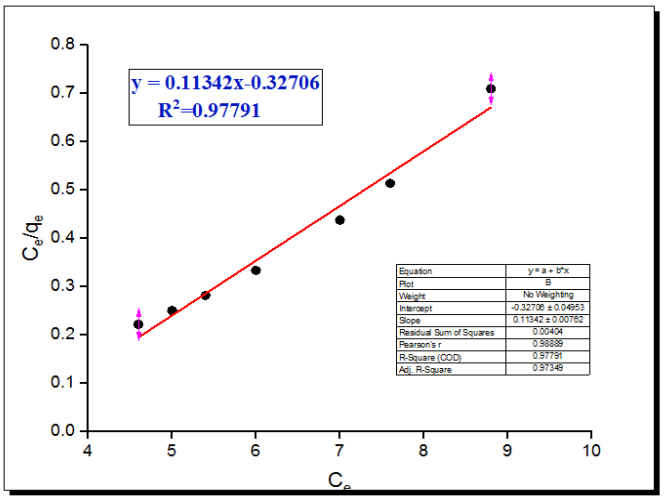

Figure 15: Langmuir Isotherm

Dubinin-Raduskevich Isotherm: It is used to determine the mechanism of adsorption[12,29]. The linearized equation is given by:

$$\ln q_e = \ln q_D - 2B_D RT \ln\left(1+\frac{1}{C_e}\right) \quad (5)$$

Plot of *In* q_e vs $RT \ln\left(1+\frac{1}{C_e}\right)$ (Figure 17) is linear which shows that the experimental data obeys Dubinin-Raduskevich isotherm.

Jovanoic Isotherm: Jovanovic model explains the adsorption behaviour on heterogeneous surfaces[34].It is expressed as:

$$\ln q_e = \ln q_{max} - K_J C_e \quad (6)$$

The linearity of the plot of C_e Vs *In* q_e (Figure 18) confirmed that the adsorption data fitted in Jovanoic model. The data obtained from isotherm studies is given in table 1.

Kinetic study: Pseudo first order and pseudo second order models[23,35] are applied for predicting kinetic sorption studies. The graphical representation is shown in figures 19 and 20.

$$\ln(q_e - q_t) = \ln q_e - k_1 t \quad (7)$$

$$\frac{t}{q_t} = \frac{1}{k_2}(q_e)^2 + \frac{t}{q_e} \quad (8)$$

Pseudo second order kinetic model was found to fit owing to higher R^2 value in pseudo second order kinetics than that of pseudo first order kinetics.

Thermodynamic study: The thermodynamic variables (ΔG◦, ΔH◦ and ΔS◦) were determined[31] using the equations:

$$\Delta G^o = -RT \ln K_L \quad (9)$$

$$\Delta G^\circ = \Delta H^\circ - T\Delta S^\circ \quad (10)$$

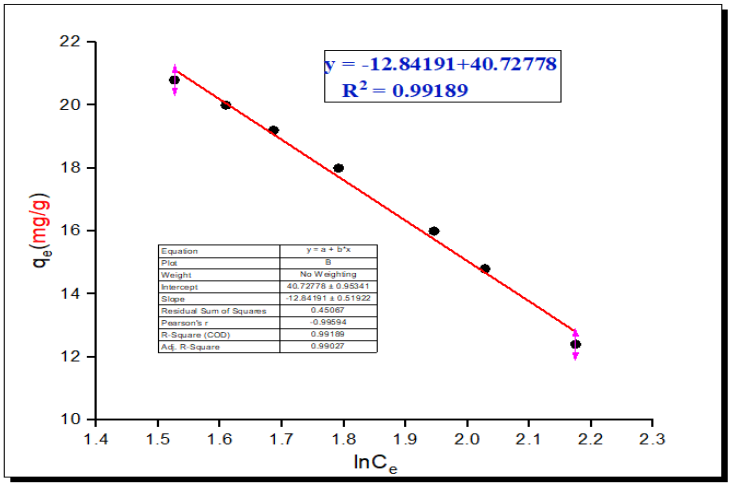

Figure 16: Temkin Isotherm

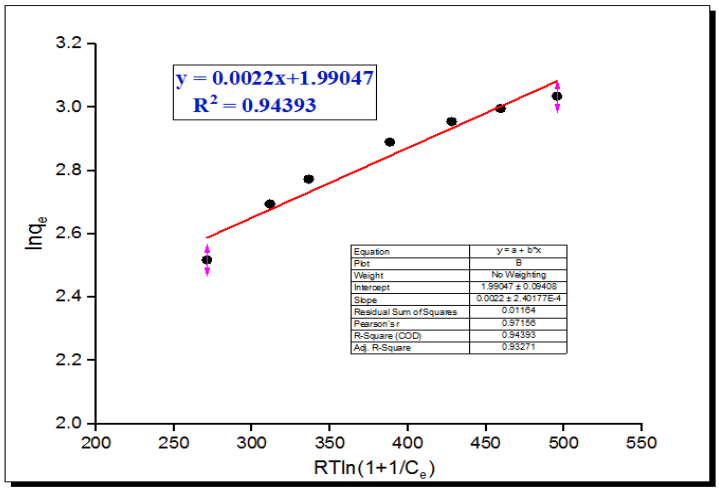

Figure 17: Dubinin-Raduskevich isotherm

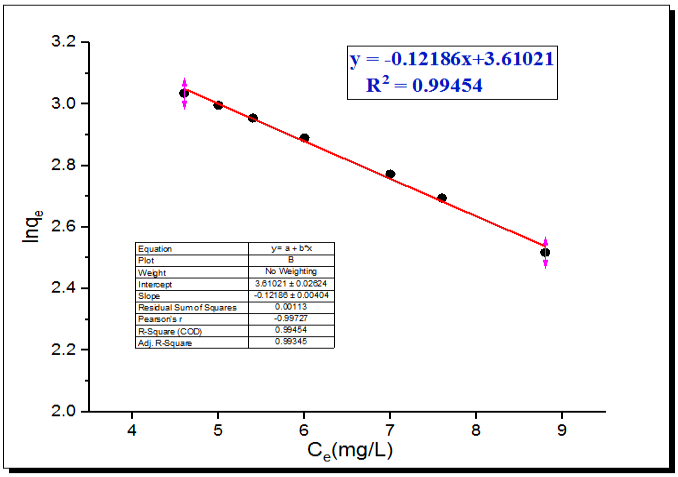

Figure 18: Jovanovic Isotherm

Table 1
Adsorption Isotherm constants

Isotherm	**Equation**	**Parameters**	**R^2**
Freundlich	$\ln q_e = \ln K_f + \frac{1}{n} \ln C_e$	$\frac{1}{n}$ =0.7773 K_f =70.4216	0.9736
Langmuir	$\frac{C_e}{Q_0} = \left(\frac{1}{Q_0 b}\right) + \left(\frac{C_e}{Q_0}\right)$	Q_0 =8.8183 b =0.3467	0.9779
Temkin	$q_e = B_T \ln K_T + B_T \ln C_e$	B_T =12.842 K_T =23.8432	0.9919
Dubinin-Raduskevich	$\ln q_e = \ln q_D - 2B_D RT \ln\left(1 + \frac{1}{C_e}\right)$	B_D =0.0011 q_D =7.3192	0.9439
Jovanoic Isotherm	$\ln q_e = \ln q_{max} - K_J C_e$	K_J =0.1219 q_{max} =36.9734	0.9945

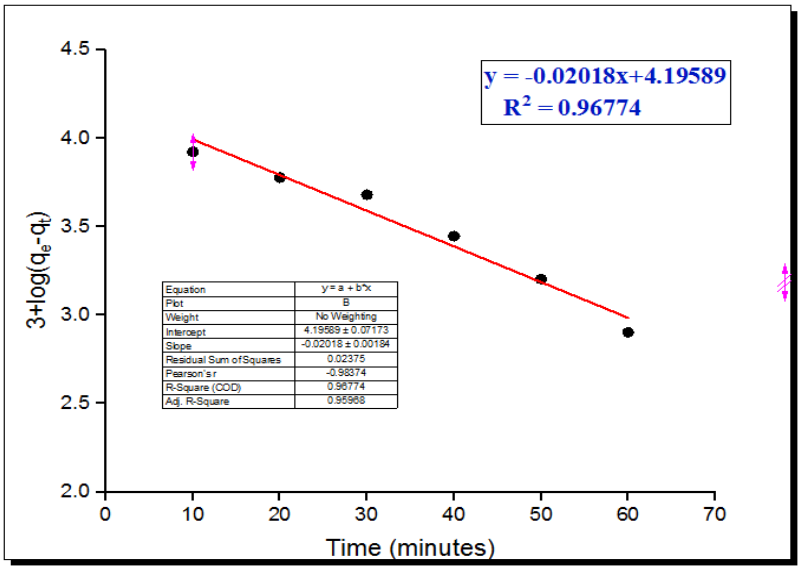

Figure 19: Pseudo first order kinetics

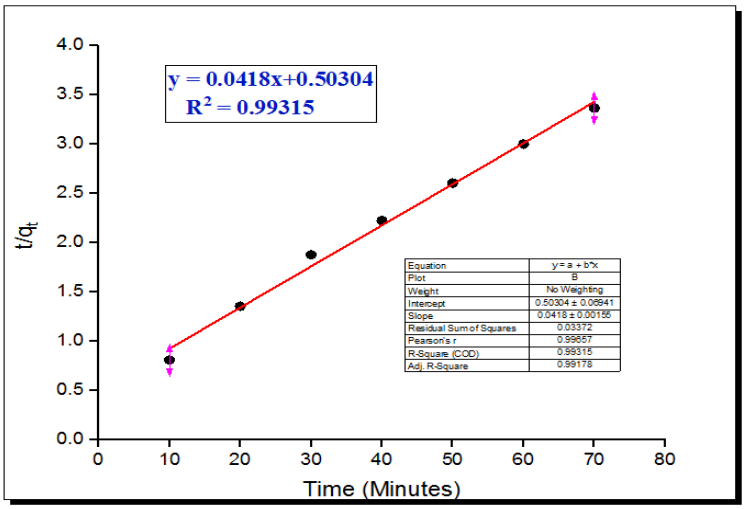

Figure 20: Pseudo second order kinetics

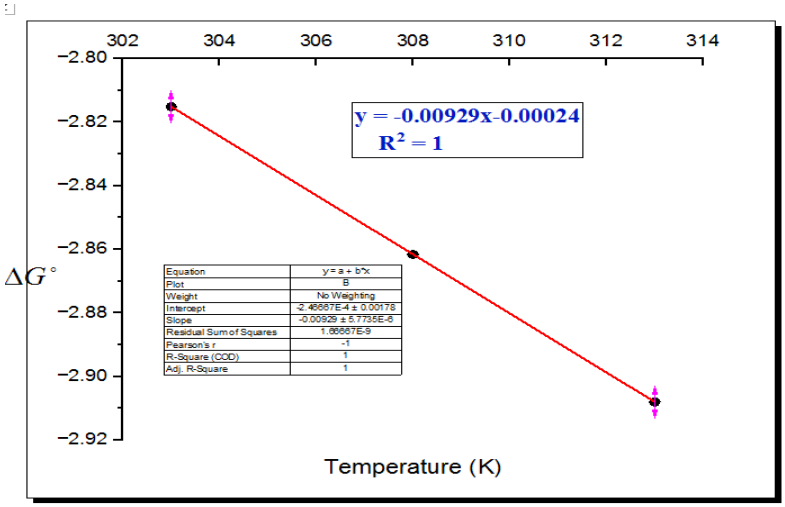

Figure 21: Thermodynamic Plot

A straight line was obtained in the plot of ΔG° versus T (Figure 21). The slope and intercept of the plot were used to calculate ΔS° and ΔH° respectively. The feasibility of process of adsorption is indicated by the negative value of ΔG° (-2.8151). The negative values of ΔH° (-0.0002) and positive value of ΔS° (+0.0093) imply that the adsorption is exothermic and displays the affinity of adsorbent towards adsorbent.

Conclusion

In the present investigation, copper oxide nanoparticles were prepared and characterized using FTIR, SEM, EDX and XRD analysis.The experimental results revealed that percentage decolourisation rises with increase in period of contact,adsorbent dosage, temperature and agitation speed and decreases with increase concentration of dye and pH of the solution. Batch adsorption obeyed Langmuir, Freundlich, Dubinin-Raduskevich, Temkin and Jovanoic isotherm. From the kinetic data, it is evident that process of adsorption follows pseudo second order kinetics and study of thermodynamics proved the exothermic, feasible and spontaneous nature of adsorption process.

References

1. Abou-Melha K.S., AI-Hazmi G.A.A., Althagafi I., Shah R., Shaaban F., El-Metwaly N.M. and El-Bindary A.A., Preparation of CuO nanoparticles via organometallic chelate for the removal of acid red 57 from aqueous solutions, *Desalination and Water Treatment*, **222**, 282-294 **(2021)**

2. Adam F.A., Ghoniem M.G., Diawara M., Rahali S., Abdulkhair B.Y., Elamin M.R., Aissa M.A.B. and Seydou M., Enhanced adsorptive removal of indigo carmine dye by bismuth oxide doped MgO based adsorbents from aqueous solution; Equilibrium, kinetics and computational studies, *Royal Society of Chemistry Advances*, **12**, 24786-24803 **(2022)**

3. Ahmad Z.U., Yao L., Lian Q., Islam F., Zappi M.E. and Gang D.D., The use of artificial neural network (ANN) for modeling adsorption of sunset yellow onto neodymium modified ordered mesoporous carbon, *Chemosphere*, **256**, 127081 **(2020)**

4. Ahmadi S., Banach A., Kord Mostafapour F. and Balarak D., Study survey of cupric oxide nanoparticles in removal efficiency of ciprofloxacin antibiotic from aqueous solution: Adsorption isotherm study, *Desalination and Water Treatment*, **89**, 297-303 **(2017)**

5. Ahmadi S. and Kord Mostafapour F., Adsorptive removal of aniline from aqueous solutions by Pistacia Atlantica (Baneh) shells: isotherm and kinetic studies, *Journal of Science, Technology and Environment Informatics*, **5**, 327-335 **(2017)**

6. AL-Niami A.D., Atiya G. and Abdulateef D., Thermodynamics and kinetic study eosin dye adsorption on CuO nanoparticles, *International Journal of Research in Pharmacy and Chemistry*, **8(2)**, 281-293 **(2018)**

7. Asha Radhakrishnan A. and Baskaran Beena B., Structural and optical absorption analysis of CuO nanoparticles, *Indian Journal of Advances in Chemical Sciences*, **2(2)**, 158-161 **(2014)**

8. Azad F.N., Ghaedi M., Asfaram A., Jamshidi A., Hassani G., Goudarzi A., Azqhandi M.H.A. and Ghaedi A., Optimization of the process parameters for the adsorption of ternary dyes by Ni doped FeO(OH)-NWs-AC using response surface methodology and an artificial neural network, *Royal Society of Chemistry Advances*, **6**, 19768-19779 **(2016)**

9. Bagheri A.R., Ghaedi M., Asfaram A., Hajati S., Ghaedi A.M., Bazrafshan A. and Rahimi M.R., Modeling and optimization of simultaneous removal of ternary dyes onto copper sulfidenanoparticles loaded on activated carbon using second – derivative spectrophotometry, *J. Taiwan Inst. Chem. Eng.*, **65**, 212-224 **(2016)**

10. Batool M., Daoush W.M., Hashmi F., Mehboob N. and Qureshi Z., Kinetic isotherm studies of azo dyes by metallic oxide nanoparticles adsorbent, *Archives of Organic and Inorganic Chemical Sciences*, **3(5)**, 426-435 **(2018)**

11. Bhaviya Raj R., Umadevi M. and Parimaladevi R., Enhanced photocatalytic degradation of textile dyeing waste water under UV and visible light using ZnO/MgO nanocomposites as a novel photocatalyst, *Particulate Science and Technology*, **38(2)**, 1-9 **(2019)**

12. Dubinin M.M., Modern state of the theory of volume filling of micropore adsorbents during adsorption of gases and steams on carbon adsorbents, *Zh. Fiz. Khim*., **39**, 1305-1317 **(1965)**

13. El Messaoudi N. et al, Desorption of Congo red from dye-loaded Phoenix dactylifera date stones and Ziziphus lotus jujube shells, *Groundwater for Sustainable Development*, **12**, 100552 **(2021)**

14. Ethiraj A. and Kang D., Synthesis and characterisation of CuO nanowires by a simple wet chemical method, *Nanoscale Res Lett*., **7(1)**, 1-5 **(2012)**

15. Franco D.S.P., Duarte F.A., Salau N.P.G. and Dotto G.L., Analysis of indium (III)adsorption from leachates of LCD screens using artificial neural networks(ANN) and adaptive neuro fuzzy inference systems(ANIFS*), J. Hazard Mater.*, **384**, 121137 **(2020)**

16. Gadekar M.R. and Ahammed M.M., Modelling dye removal by adsorption onto water treatment residuals using combined response surface methodology –artificial neural network approach, *J. Environ. Manage*., **231**, 241-248 **(2019)**

17. Hammed B.H., Chin L.H. and Rengaraj S., Adsorption of 4-chlorophenol onto activated carbon prepared from rattan sawdust, *Desalination*, **225**, 185-198 **(2008)**

18. Iqbal M. and Saeed A., Biosorption of reactive dye by loofe sponge immobilised fungal biomass of phanerochaete chrysosporium, *Process Biochem*., **42**, 1160-1164 **(2007)**

19. Kapdan I.K. and Kargi F., Simultaneous biodegradation and adsorption of textile dye stuff in an activated sludge unit, *Process Biochemistry*, **37**, 973-998 **(2002)**

20. Karthika M. and Vasuki M., Adsorption of Alizarine Red-S Dye from Aqueous Solution by Cane Sugar Bagasse: Resolution of Isotherm, Kinetic and Thermodynamics, *International Journal of Applied Engineering Research*, **13(12)**, 10260-10267 **(2018)**

21. Khan M.M.R., Mukilish M.Z.B., Mazumder M.S.I., Ferdous K., Prasad D.M.R. and Hassan Z., Uptake of indosol dark-blue GL dye from aqueous solution by water hyacinth roots powder: Adsorption and desorption study, *Int. J. Environ. Sci. Technol.*, **11**, 1027-1034 **(2014)**

22. Khosla E., Kaur S. and Dave P., Mechanistic study of adsorption of acid orange-7 over aluminium oxide nanoparticles, *Journal of Engineering*, **1**, 1-8 **(2013)**

23. Kul A.R. and Koyuncu H., Adsorption of Pb (II) ions from aqueous solution by native and activated bentonite: kinetic, equilibrium and thermodynamic study, *J. Hazard Mater.*, **179(1)**, 332-339 **(2010)**

24. Mulugeta M. and Belisti L., Removal of methylene blue dye from aqueous solution by bioadsorption onto untreated Parthenium hystrophorus weed, *Modern Chemistry Applications*, **2**, 1-15 **(2014)**

25. Naghizade Asl M., Mahmodi N.M., Teymouri P., Shamoradi B., Rezaee R. and Maleki A., Adsorption of organic dyes using copper oxide nanoparticles: isotherm and kinetic studies, *Desalination and Water Treatment*, **57(52)**, 25278-25287 **(2016)**

26. Nanta P., Kasemwong K. and Skolpap W., Isotherm and kinetic modelling on superparamagnetic nanoparticles adsorption of polysachharide, *J. Environ Chem Eng.*, **6(1)**, 794-802 **(2018)**

27. Panigrahi Rajashree and Parida Reena, Rapid multiplication of Zingiber cassumunar using axillary bud explant, *Res. J. Biotech*., **19(5)**, 47-50 **(2024)**

28. Qingdong Q., Sun T., Yin W. and Xu Y., Rapid and efficient removal of methylene blue by freshly prepared manganese dioxide, *Cogent Engineering*, **1**, 1-10 **(2017)**

29. Radushkevich L.V., Potential theory of sorption and structure of carbons, *Zh. Fiz. Khim*., **23**, 1410-1420 **(1949)**

30. Rangel W.M., Antunes Boca Santa R.A. and Riella H.G., A facile method for synthesis of nanostructured copper (II) oxide by coprecipitation, *Journal of Materials Research and Technology*, **9(1)**, 994-1004 **(2020)**

31. Rashad M. and Hatem A. Al-Aoh., Promising adsorption studies of bromophenol blue using copper oxide nanoparticles, *Desalination Water Treatment*, **139**, 360-368 **(2019)**

32. Rathinam A., Nishatar N., Johnalagadda R. and Balachandran U., Equilibrium and thermodynamic studies on the removal of

basic black dye using calcium alginate beads, *Colloids and surfaces A: Physicochem. Eng. Aspects*, **299**, 232-238 **(2007)**

33. Samadi M.T., Kashitarash E.Z., Ahangari F., Ahmadi Sh. and Jafari J., Nickel removal from aqueous environments using carbon nanotubes, *Water and Waste Water*, **24**, 38-44 **(2013)**

34. Shahbeig H., Bagheri N., Ghorbanian S.A., Hallajisani A. and Poorkarimi S., A new adsorption isotherm model of aqueous solution of granular activated carbon, *World Journal of Modelling and Simulation*, **9(4)**, 243-254 **(2013)**

35. Temkin M. and Pyzhev V., Kinetics of ammonia synthesis on promoted iron catalyst, *Acta Physio chim URSS*, **12**, 327-352 **(1940)**

36. Venkata Ratnam M., Meena Vangalapati, Nagamallaeswara Rao K. and Ramesh Chandra K., Efficient removal of methyl orange using magnesium oxide nanoparticles loaded onto activated carbon, *Bull. Chem. Soc. Ethiopia.*, **36(3)**, 531-544 **(2022)**.

(Received 19th January 2025, accepted 21st February 2025)